



**Fermi National Accelerator Laboratory**

**FERMILAB-Pub-91/75-E**  
**[E687]**

## **A Measurement of the $D^0$ and $D^+$ Lifetimes\***

**E687 Collaboration**  
*Fermi National Accelerator Laboratory*  
*P. O. Box 500*  
*Batavia, Illinois 60510*

**March 1991**

\* To be submitted to Phys Lett.



**Operated by Universities Research Association Inc. under contract with the United States Department of Energy**

# A Measurement of the $D^0$ and $D^+$ Lifetimes

P.L. Frabetti

*Dip. di Fisica dell'Universita' and INFN - Bologna, I-40126 Bologna, Italy*

C.W. Bogart<sup>a</sup>, H.W.K. Cheung, S. Culy, J.P. Cumalat  
*University of Colorado, Boulder, CO 80309, USA*

J.N. Butler, F. Davenport<sup>b</sup>, I. Gaines, P.H. Garbincius, S. Gourlay, D.J. Harding,  
P. Kasper, A. Kreymer, P. Lebrun, H. Mendez<sup>c</sup>  
*Fermilab, Batavia, IL 60510, USA*

S. Bianco, M. Enorini, F.L. Fabbri, A. Spallone, A. Zallo  
*Laboratori Nazionali di Frascati dell'INFN, I-00044 Frascati, Italy*

R. Culbertson, G. Jaross<sup>d</sup>, K. Lingel<sup>e</sup>, P.D. Sheldon, J.R. Wilson<sup>f</sup>, J. Wiss  
*University of Illinois at Urbana-Champaign, Urbana, IL 61801, USA*

G. Alimonti, G. Bellini, M. Di Corato, M. Giammarchi, P. Inzani, S. Malvezzi,  
P.F. Manfredi<sup>g</sup>, D. Menasce, L. Moroni, D. Pedrini, L. Perasso, A. Sala, S. Sala,  
D. Torretta, M. Vittone<sup>h</sup>

*Dip. di Fisica dell'Universita' and INFN - Milano, I-20133 Milan, Italy*

D. Buchholz, C. Castoldi<sup>i</sup>, B. Gobbi, S. Park<sup>k</sup>, R. Yoshida<sup>j</sup>  
*Northwestern University, Evanston, IL 60208, USA*

J.M. Bishop, J.K. Busenitz<sup>k</sup>, N.M. Cason, J.D. Cunningham<sup>l</sup>, R.W. Gardner,  
C.J. Kennedy, E.J. Mannel, R.J. Mountain, D.L. Pusejic, R.C. Ruchti,  
W.D. Shephard, M.E. Zanabria  
*University of Notre Dame, Notre Dame, IN 46556, USA*

S.P. Ratti, P. Vitulo

*Dip. di Fisica Nucleare dell'Universita' and INFN - Pavia, I-27100 Pavia, Italy*

A. Lopez

*University of Puerto Rico at Mayaguez, Puerto Rico*

We present precision measurements of the  $D^0$  and  $D^+$  meson lifetimes using approximately 7500 fully reconstructed  $D^0 \rightarrow K^-\pi^+$ ,  $K^-\pi^+\pi^+\pi^-$ ,  $D^+ \rightarrow K^-\pi^+\pi^+$ , and charge conjugate decays. The data were accumulated by the Fermilab high energy photoproduction experiment E687. The lifetime of the  $D^0$  is measured to be  $0.424 \pm 0.011 \pm 0.007$  picoseconds while the  $D^+$  lifetime is measured to be  $1.075 \pm 0.040 \pm 0.018$  picoseconds.

We report on precision measurements of the  $D^0$  and  $D^+$  lifetime using data collected in the Fermilab wideband photoproduction experiment E687. The E687 detector is a multiparticle magnetic spectrometer with excellent vertex measurement, particle identification, and calorimetric capabilities. The apparatus is described in detail elsewhere.<sup>1</sup> Charged particles emerging from the experimental target are tracked through a twelve plane silicon microstrip vertex detector, an analysis magnet, three stations of multiwire proportional chambers, a second analysis magnet, and two more multiwire proportional stations. Three Cerenkov counters with different thresholds allow kaons to be separated from pions over a momentum range from 4.5 to 61 GeV.

The photon beam, also described in Reference 1, is derived from electrons of 350 GeV/c momentum with a  $\pm 13\%$  momentum bite. These electrons impinge on a 27% radiator producing a bremsstrahlung photon beam. The photon beam is tagged by detection of the recoil electron and interacts in a 12% interaction length Be target<sup>2</sup>. The trigger required a radiated energy loss between the incident and recoil electron exceeding 130 GeV, a minimum 35 GeV hadronic energy deposition in the hadron calorimeter, and the presence of at least two charged tracks in the spectrometer (both of which had to be outside the pair production region). The average tagged photon energy for this data sample was 221 GeV. Approximately 60 million triggers were recorded on tape during the experiment. The results presented in this work are based on a sample of approximately 7500 fully reconstructed  $D^0$  and  $D^+$  decays, divided nearly equally among the decay modes  $K^-\pi^+$ ,  $K^-\pi^+\pi^+\pi^-$ , and  $K^-\pi^+\pi^-$ . Throughout this paper, the charge conjugate state is implied when a decay mode of a specific charge is stated.

The silicon microstrip planes which comprise the vertex detector are divided transversely. The inner region has half the strip spacing of the outer regions. Most of the secondary tracks from charmed particle decays have at least 3/4 of their hits in the inner, high resolution region. For such tracks, the transverse extrapolated position resolutions at the target plane are given by:

$$\sigma_x = 11\mu m \sqrt{1 + \left(\frac{17.5 \text{ GeV}}{p}\right)^2}$$

$$\sigma_y = 7.7\mu m \sqrt{1 + \left(\frac{25 \text{ GeV}}{p}\right)^2}$$

The secondary vertices from accepted  $D$  decays are measured with a longitudinal uncertainty of  $\sigma_l \approx 5.3 \times P_D \mu m$ , where  $P_D$  is the momentum (in GeV/c) of the decaying  $D$ . Uncertainties in locating the primary vertex contribute comparable errors to the determination of the decay length.

Two complementary approaches are used to skim and analyze the charm sample based on the presence of a downstream decay vertex. These are called the “candidate driven” vertex method and the “stand alone” vertex method.<sup>1</sup> We begin with a discussion of the approach which uses a candidate driven vertex finder to search for  $D$  decays into specific all-charged decay modes. In this technique, the charmed particle candidate is *assumed* to form a secondary vertex. A “seed” track which passes through the secondary vertex and is directed along the  $D$  candidate’s momentum vector is used to search for the primary vertex. The vertex finder reconstructs the primary vertex by searching for tracks which form high confidence level intersections with the seed track. Proper cognizance is taken of the track and seed track parameter errors. Tracks are added to the primary vertex as long as the confidence level of the resultant vertex exceeds 2%. The efficiency of this algorithm in finding primary vertices is essentially independent of the primary and secondary ( $D$ ) vertex separation. This algorithm does not suffer from a loss of efficiency at small separations which can create a bias in lifetime measurements.

To obtain the  $K\pi$ ,  $K3\pi$  and  $K2\pi$  charm signals, we used the following cuts. Each of the decay secondaries is required to form an acceptable track in both the microstrip and multiwire proportional chamber systems and the two sets of track parameters must be consistent within measurement errors. No Cerenkov criteria are applied to the pions. Kaon candidates with a momentum below 61 GeV/c are required to have a Cerenkov light pattern consistent with that expected for charged kaons but inconsistent with pions, muons, and electrons. Kaon candidates with momenta above 61 GeV/c are only required to have a light pattern consistent with that of a charged kaon, although totally confused cases are rejected. The charge and strangeness of the secondaries are required to exhibit the correlations expected for Cabibbo allowed charmed particle decays.

The microstrip segments of all tracks which comprise a secondary vertex are required to extrapolate back to a single point with a confidence level exceeding 1%. We require that the secondary vertex lies upstream of the first microstrip plane in order to reduce systematic effects due to inefficient track reconstruction for charmed particles decaying within the microstrip system. The final important cut is on the significance of the detachment between the primary and secondary vertex. We cut on the variable  $\ell/\sigma_\ell$ , where  $\ell$  is the signed 3 dimensional separation between the vertices, and  $\sigma_\ell$  is the error on  $\ell$  computed on an event by event basis including the effects of multiple coulomb scattering. Results are reported for a series of detachment cuts ranging from  $\ell/\sigma_\ell > 0$  to  $\ell/\sigma_\ell > 20$ .

To provide consistency checks and maximize signal to noise, we consider two sources of  $D^0$ ’s in this analysis. The first source, which we will call the “ $D^*$ -tag” sample, con-

sists primarily of  $D^0$ 's from the decay chain  $D^{*+} \rightarrow \pi^+ D^0$  with the  $D^0$  subsequently decaying into either the  $K\pi$  or  $K3\pi$  topology. A  $D$  is placed into the  $D^*$ -tag sample if a "soft" pion of the correct charge can be combined with the  $D^0$  such that the  $M(D^0\pi^+) - M(D^0)$  invariant mass difference lies within  $\pm 2 \text{ MeV}/c^2$  of the accepted<sup>3</sup> mass difference. In order to increase acceptance and reduce momentum biases, the soft pion is only required to be reconstructed in the multiwire proportional system, and is not required to have a reconstructed segment in the microstrips. The second sample, called the "no-tag" sample, consists of those events which satisfy the vertex and particle identification cuts described above but have no soft pion within the acceptance which is consistent with the  $D^* - D^0$  cascade hypothesis. These two samples are therefore statistically independent. Figure 1 shows invariant mass distributions for the four  $D^0$  samples and the one  $D^+$  sample described above. For each sample, we use the minimum vertex detachment ( $\ell/\sigma_\ell$ ) cut which results in a peak height roughly equal to the background level. We require  $\ell/\sigma_\ell$  to be greater than 0, 5, 2, 7, and 5 for the  $K\pi$   $D^*$ -tag,  $K\pi$  no-tag,  $K3\pi$   $D^*$ -tag,  $K3\pi$  no-tag, and  $K2\pi$   $D^+$  samples, respectively. The charm signal yields, presented with the figures, are deduced from fits to the mass distributions of a Gaussian peak over a polynomial background.

In order to measure the  $D$  lifetimes we use a variant of the fitting procedure used in Reference 4. We fit to the *reduced proper time* distribution. The reduced proper time variable ( $t'$ ) is defined as  $t' = (\ell - \mathcal{N}\sigma_\ell)/\beta\gamma c$ , where  $\mathcal{N}$  represents the significance of vertex detachment cut ( $\ell/\sigma_\ell > \mathcal{N}$ ), and  $\beta\gamma$  is the lab frame Lorentz boost parameter of the  $D$ . To the extent that  $\sigma_\ell$  is independent of  $\ell$  (as Monte Carlo studies show), the  $t'$  distribution for decaying  $D$ 's will be of the form  $\exp(-t'/\tau)$  where  $\tau$  is the  $D$  lifetime.

A fit is made to the  $t'$  distribution for events within a signal region which lie within  $2\sigma$  of the  $D$  mass ( $\pm 0.030 \text{ GeV}/c^2$  for the  $K\pi$ ,  $\pm 0.020 \text{ GeV}/c^2$  for the  $K3\pi$ , and  $\pm 0.023 \text{ GeV}/c^2$  for the  $K2\pi$ ). We use a binned maximum likelihood fit in which the predicted number of events ( $n_i$ ) within a reduced proper time bin (centered at  $t'_i$ ) is a function of the charmed particle lifetime ( $\tau$ ) given by:

$$n_i = S \frac{f(t'_i) e^{-t'_i/\tau}}{\sum f(t'_i) e^{-t'_i/\tau}} + Bb_i \quad (1)$$

where  $S = N - B$ ,  $N$  is the total number of events in the signal mass region,  $B$  is the total number of background events in the signal mass region,  $b_i$  is the time evolution of the background as measured from mass sidebands ( $\sum b_i = 1$ ), and  $f(t')$  is a correction function. Twenty-five time bins are used to span six nominal lifetimes. The fit parameters are  $B$  and  $\tau$ .

The function  $f(t')$ , derived from Monte Carlo simulation, corrects the signal lifetime evolution for the effects of acceptance, skim and analysis cut efficiency, hadronic

absorption and decay of charm secondaries. Figure 2 shows plots of  $f(t')$  for the  $D^0$  and  $D^+$  samples shown in Figure 1. Very little  $f(t')$  variation is present except in the  $K2\pi$  mode. The background lifetime evolution ( $b_i$ ) is obtained from events in low mass and high mass sidebands. Each sideband has the same width as the signal region and is separated from the signal region by a gap of twice the mass resolution.

In order to tie the value of  $B$  to the background level expected from the mass sidebands, we include an additional term<sup>5</sup> in the log likelihood function. The background level is thereby jointly determined from the invariant mass plot and the lifetime evolution. Simulations show that the inclusion of this additional term significantly reduces the statistical errors of the fit. Simulations where care was made in modeling the background lifetime evolution also revealed both the presence of small biases in the lifetime fitting procedure, and a slight underestimation of the true statistical error due to neglected fluctuations in  $b_i$ . The fitting biases are found to be  $\approx .005$  ps for the  $D^0$  no-tag samples and  $\approx .003$  ps for the  $D^+$  sample.<sup>6</sup>

In Figure 3 the fit lifetime is plotted versus  $\ell/\sigma_\ell$  cut for the 4 independent  $D^0$  samples and the single  $D^+$  sample. The results are corrected for the fit biases. The statistical error bars from the fits are corrected to include contributions from fluctuations in  $b_i$  and fluctuations in  $f(t')$  due to Monte Carlo counting statistics. In choosing the  $\ell/\sigma_\ell$  points at which to quote the lifetime, we are guided by the principle of maintaining a reasonable signal to noise while keeping statistical error to a minimum. We will quote the lifetime at the  $\ell/\sigma_\ell$  cuts listed above and used for Figure 1. The results do not change significantly if we make these  $\ell/\sigma_\ell$  cuts at other reasonable values. Figure 4 shows the background subtracted, and  $f(t')$  corrected time evolution for the five charm samples. The superimposed curve is a pure exponential function using the charm lifetime found by the fit.

Performing a weighted average of the 4 independent  $D^0$  lifetime measurements with statistical errors only, we obtain a  $D^0$  lifetime of  $0.424 \pm 0.011$  ps. The confidence level for the hypothesis that the four  $D^0$  lifetime measurements are consistent within statistical errors is 24%. The  $D^+$  lifetime is measured to be  $1.075 \pm 0.040$  ps.

We now turn to a discussion of systematic errors. Due to uncertainties in the target absorption corrections, we include systematic errors of 0.0035 ps for the  $D^0$  lifetime (averaged over  $K\pi$  and  $K3\pi$ ) and 0.01 ps for the  $D^+$ . Two effects are present: hadronic absorption of decay secondaries which tends to increase the fitted  $D$  lifetime, and absorption of the  $D$  by the target material prior to decay which tends to decrease the apparent  $D$  lifetime. Uncertainty in the secondary absorption correction arises since we are unsure to what extent elastic scattering of charm secondaries causes severe mismeasurement of the parent  $D$ . The  $D$  absorption cross section is uncertain since the  $D$  - nuclear cross section has never been measured. We assume that the

pion - nuclear absorption cross section serves as a reasonable upper bound.

We ascribe an additional 0.005 ps systematic uncertainty in the  $D^+$  lifetime due to uncertainties in the  $D^+$  momentum spectrum. High momentum  $D^+$ 's have a finite probability of failing the cut requiring the charmed particle secondaries to verticize upstream of the first microstrip plane.

Charmed particles produced near the edge of the experimental target have a larger probability of lying outside the transverse fiducial volume of the first microstrip station. This effect is diminished for long lived charmed particles thus creating a lifetime bias. Uncertainties in the transverse beam profile were due primarily to running condition instability, and create an additional .002 ps systematic uncertainty in both charged and neutral  $D$  lifetimes.

Finally, we attribute a systematic uncertainty of about .006 ps<sup>7</sup> to the lifetime of the  $D^0$  and .009 ps to the lifetime of the  $D^+$  due to uncertainties in the background time evolution. These uncertainties were determined by comparing the lifetime results from fits which used varying weighted averages of the high mass sideband and the low mass sideband. Both the fitted lifetime, and the  $\chi^2$  of the fitted lifetime evolution were tracked as the high mass sideband fraction was varied from 0 to 1. The background systematic error is determined from the spread of lifetime estimates consistent with a  $\chi^2$  increase of one from the  $\chi^2$  minimum. In all cases where a significant  $\chi^2$  change was observed, the  $\chi^2$  minimum was consistent with equal weighting of the high and low mass sideband.

Combining all sources of systematic error<sup>8</sup> we obtain a final lifetime measurement of  $0.424 \pm 0.011$  (statistical)  $\pm .007$  (systematic) ps for the  $D^0$  and  $1.075 \pm 0.040 \pm .018$  ps for the  $D^+$ . The present world average<sup>3</sup> is  $0.421 \pm 0.010$  ps for the  $D^0$  and  $1.062 \pm .028$  ps for the  $D^+$ .

We next discuss the results of an analysis based on the "stand alone" vertex method. The use of an alternative approach allows us to estimate the sensitivity of our result to the vertex algorithm itself, since the two methods have very different sources of systematic error. In the stand alone approach, the vertex finder iteratively intersects tracks to search for events containing more than one cleanly isolated vertex. The charm signals obtained with the stand alone vertex finder are very clean. However, this algorithm is inefficient at short decay times.

Figure 5 shows the  $D^0$  and  $D^+$  charm signals used in this alternative analysis. To enter into Figure 5, the secondaries from a charm candidate must lie in a single, isolated vertex which includes no additional tracks. An upstream primary vertex must be found which lies within the target region. The momentum vector of the  $D$  candidate when extrapolated back from the secondary vertex must point to the primary vertex within a transverse distance of less than 60  $\mu\text{m}$ . The candidate must

possess the strangeness and charge correlations expected for the Cabibbo favored decays of a charmed particle. Cerenkov requirements on the kaon are the same as in the first analysis. In addition, particles identified as kaons or protons are rejected as pion candidates.

Lifetimes were computed from a binned likelihood fit to the proper time<sup>9</sup> evolution of candidates with masses falling in the signal region ( $\pm 0.030$  GeV). The number of predicted events is again given by Equation (1) but the reduced proper time  $t'$  is replaced throughout by the proper time  $t$ ,  $B$  is fixed by the sidebands, and  $S$  and  $\tau$  are the fit parameters. The Monte Carlo correction functions used in this analysis are shown in Figure 6. The lifetimes obtained are  $0.445 \pm .020 \pm .024$  ps for the inclusive  $D^0 \rightarrow K\pi$ ,  $0.458 \pm .018 \pm .050$  ps for the inclusive  $D^0 \rightarrow K3\pi$ , and  $1.080 \pm .050 \pm .040$  ps for the  $D^+ \rightarrow K2\pi$ . The systematic error in this approach is larger because the inefficiency at short lifetimes is a more serious source of systematic error than the uncertainty in subtracting the (larger) background of the candidate driven approach. A rough estimate of the systematic error due to uncertainties in the  $f(t)$  function is obtained by comparing the consistency of lifetime estimates from fits which use only small proper time candidates in the region where  $f(t)$  is varying rapidly, and fits which use only long proper time candidates in the region where  $f(t)$  is nearly constant. A relatively small contribution due to background systematics is added in quadrature. From a combined fit to the two neutral  $D^0$  modes, a lifetime of  $0.450 \pm .012 \pm .037$  ps is obtained.<sup>10</sup> These results are clearly consistent with the results of the previously discussed candidate driven analysis once systematic as well as statistical errors are considered.<sup>11</sup>

In summary, we report on new measurements of the  $D^0$  and  $D^+$  lifetime based on a sample of  $\approx 7500$  reconstructed decays into the modes  $K\pi$ ,  $K3\pi$ , and  $K2\pi$ . The lifetime of the  $D^0$  is measured to be  $0.424 \pm 0.011$  (statistical)  $\pm 0.007$  (systematic) ps while the  $D^+$  lifetime is measured to be  $1.075 \pm 0.040 \pm 0.018$  ps. The data satisfy several internal consistency checks including consistency between the  $K\pi$  and  $K3\pi$   $D^0$  modes and consistency between the  $D^*$  tag and no-tag  $D^0$  samples. Two analyses based on completely different vertex finding and data reduction strategies yield consistent  $D^0$  and  $D^+$  lifetimes.

We wish to acknowledge the assistance of the staffs of Fermilab and I.N.F.N. Further we wish to thank the physics departments of Bologna University, University of Colorado, University of Illinois, Milano University, Northwestern University, University of Notre Dame, and Pavia University. This research was supported in part by the National Science Foundation, the U.S. Department of Energy, the Italian Istituto Nazionale di Fisica Nucleare and Ministero della Universita' e della Ricerca Scientifica.



- 
- <sup>a</sup>Present address: Vector Research Company, 6903 Rockledge Drive, Bethesda, MD 20817, USA.
- <sup>b</sup>Present address: University of North Carolina-Asheville, Asheville, NC 28804, USA.
- <sup>c</sup>Present address: Cinvestav-IPN, A.P. 14-740, 07000 Mexico DF, Mexico.
- <sup>d</sup>Present address: STX Inc., 4400 Forbes Blvd., Lanham, MD 20706
- <sup>e</sup>Present address: University of Colorado, Boulder, CO 80309
- <sup>f</sup>Present address: University of South Carolina, Columbia, SC 29208, USA.
- <sup>g</sup>Present address: Dipartimento di Elettronica, Università di Pavia, Pavia, Italy.
- <sup>h</sup>Present address: Fermilab, Batavia, IL 60510, USA.
- <sup>i</sup>Present address: INFN - Pavia, I-27100 Pavia, Italy.
- <sup>j</sup>Present address: NIKHEF-H, 1009 DB, Amsterdam, The Netherlands.
- <sup>k</sup>Present address: University of Alabama, Tuscaloosa, AL 35487, USA.
- <sup>l</sup>Present address: Brandeis University, Waltham, MA 02254, USA.
- <sup>1</sup>P.L. Frabetti *et al.*, "Description and Performance of the E687 Spectrometer", FERMILAB Pub-90/258E (1990), submitted to Nuclear Instruments and Methods.
- <sup>2</sup>Approximately 13% of the data was taken with an active Si - Be composite target.
- <sup>3</sup>M. Aguilar-Benitez *et al.* (Particle Data Group), Phys. Lett. **B239**, 1 (1990).
- <sup>4</sup>J.R. Raab *et al.*, Phys. Rev. **D37**, 2391 (1988).
- <sup>5</sup>The additional term is the logarithm of the Poisson probability for finding the observed number events in the combined mass sidebands when the expected number is  $2B$ .
- <sup>6</sup>Except for fits to samples with  $\ell/\sigma_\ell$  cuts beyond 15 where the biases become up to two times larger.
- <sup>7</sup>This represents the average background systematic error over all four neutral D samples.
- <sup>8</sup>In combining the systematic errors we make the conservative assumption that the absorption, beam profile, and upstream microstrip cut are completely correlated. We assume that the background systematic error is correlated between the  $D^*$ -tag and no-tag samples of a specific  $D^0$  topology, but is uncorrelated with other systematic sources.
- <sup>9</sup>As opposed to the *reduced* proper time variable employed in the previously discussed analysis.
- <sup>10</sup>To be conservative, we have averaged the above estimates of the  $K\pi$  and  $K3\pi$  systematic errors.
- <sup>11</sup>By searching for events common to both data samples we have computed that the statistical correlation between the two analyses is expected to lie in the range 30-60%.

FIG. 1.  $D^0$  and  $D^+$  signals used in the candidate driven lifetime analysis with the indicated decay mode and signal peak yield. The fit masses are within 2.5 MeV of the current world averages<sup>3</sup> and the widths of the signals are consistent with our experimental resolution.

FIG. 2. The deviation from a pure exponential decay (  $f(t')$  ) computed from Monte Carlo simulations for the five charm samples.  $\tau$  is the appropriate charm lifetime.

FIG. 3. Results of lifetime fits as a function of  $\ell/\sigma_\ell$  cut for the four  $D^0$  and  $D^+$  samples. Both the lifetimes and statistical error bars have been corrected for the background effects described in the text.

FIG. 4. The background subtracted and Monte Carlo corrected lifetime evolution measured for the five charm samples.

FIG. 5. Charm signals used for the stand alone vertex finder analysis.

FIG. 6. Monte Carlo correction functions  $f(t)$  appropriate for the stand alone vertex finder analysis.

Figure 1

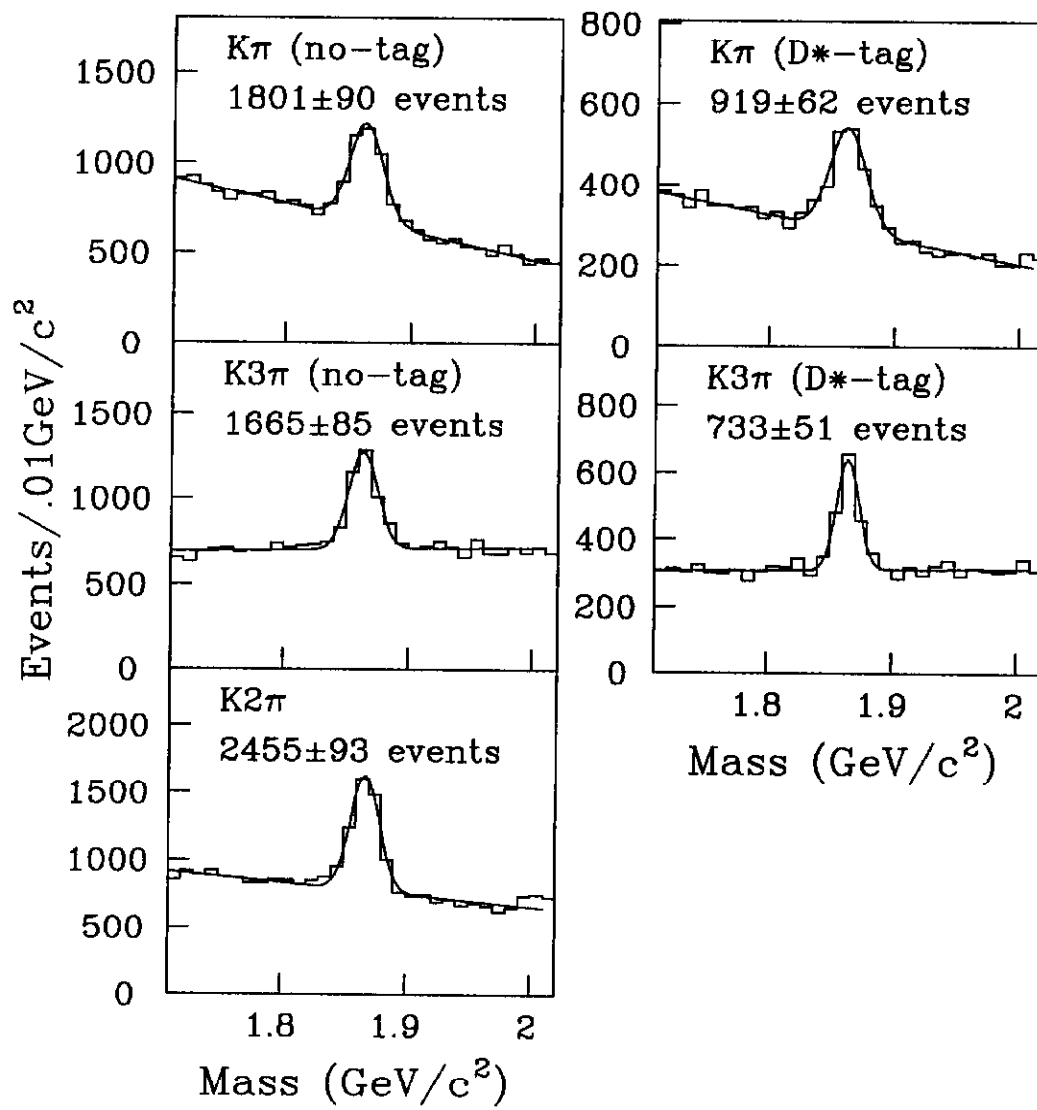


Figure 2

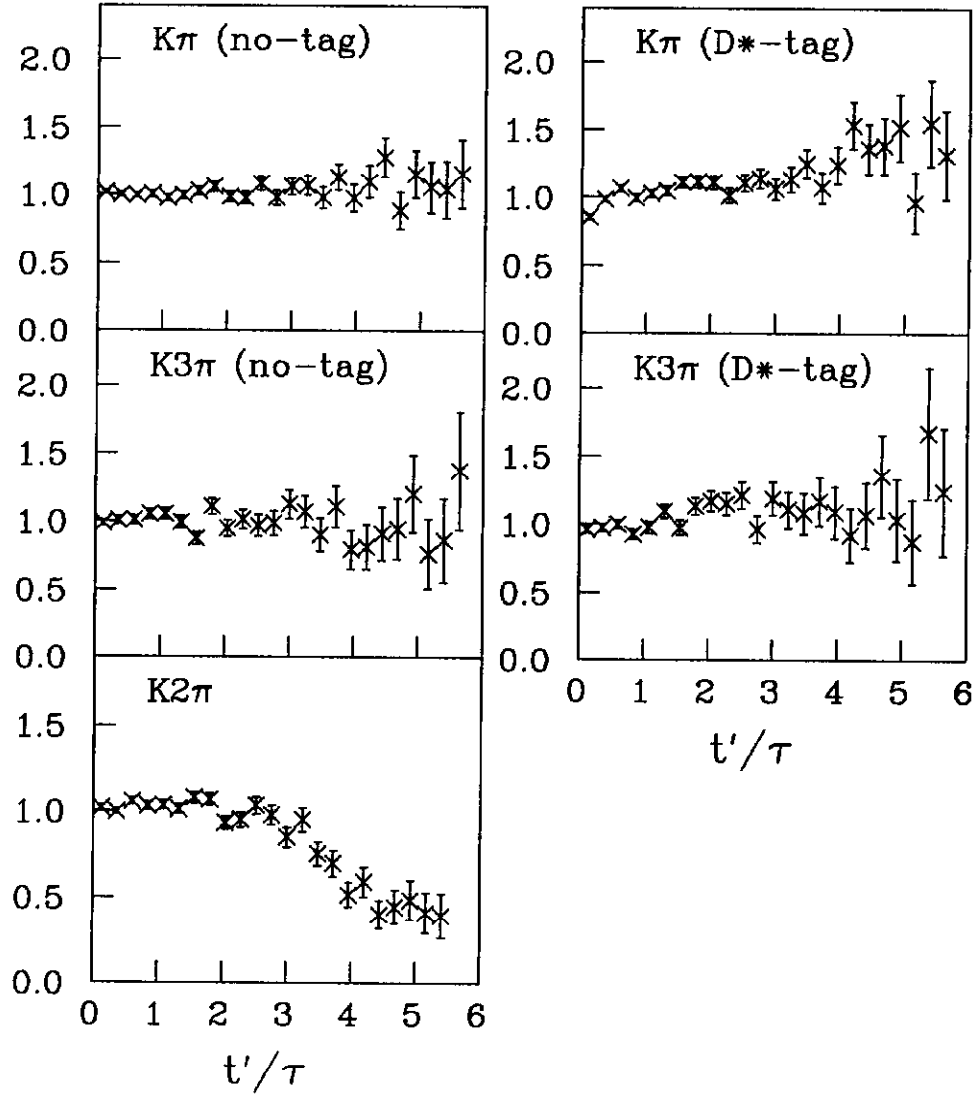
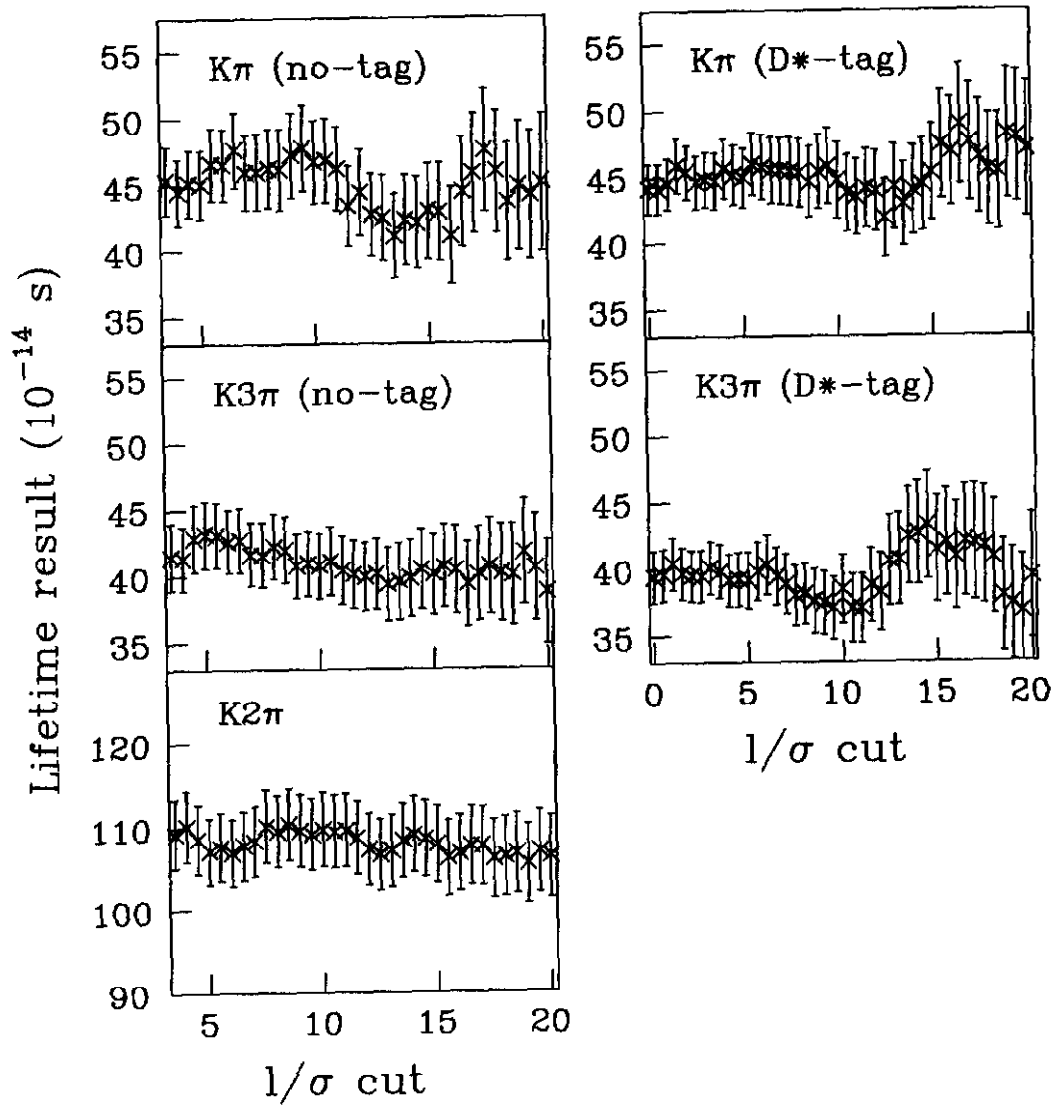


Figure 3



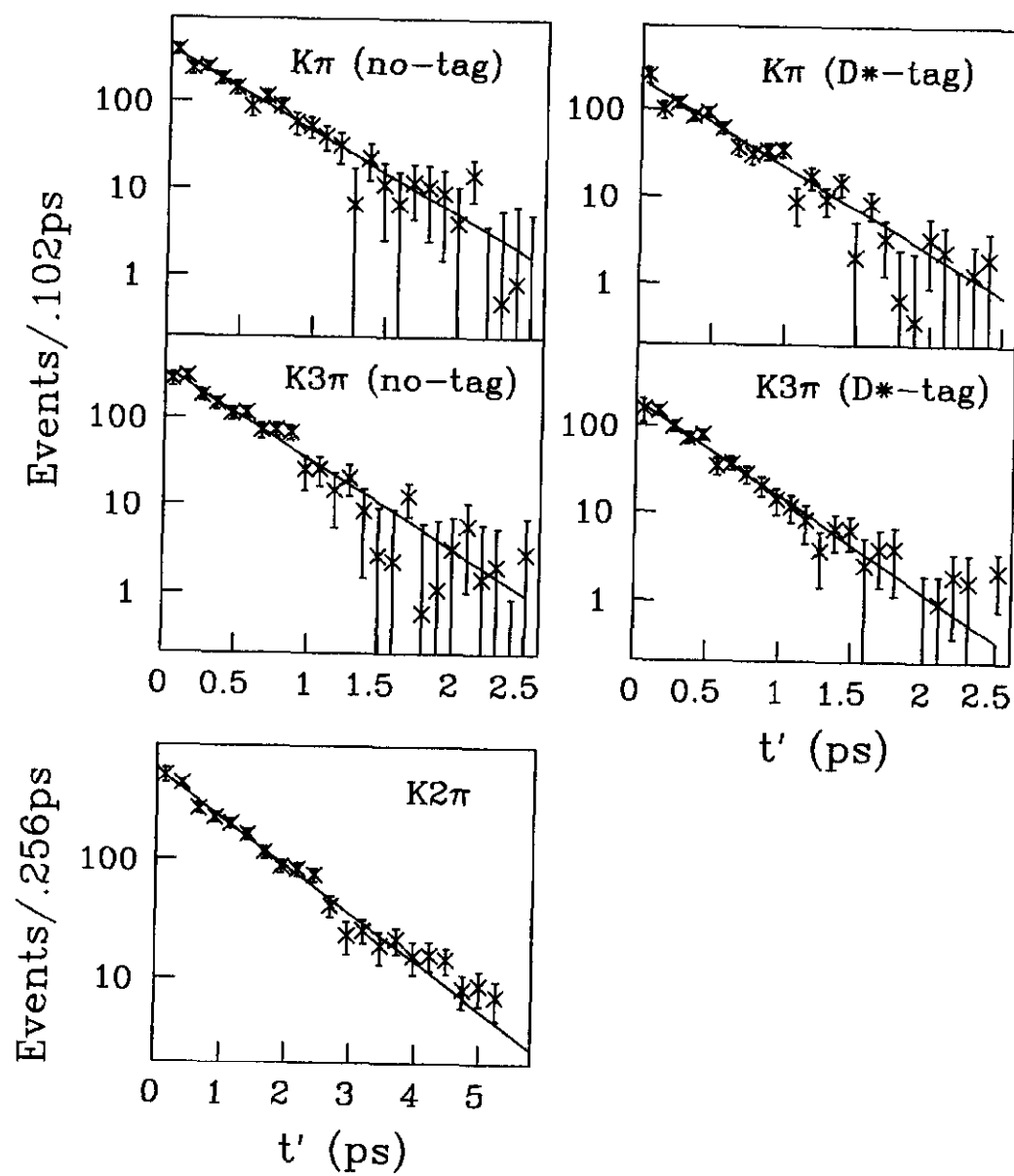


Figure 4

Figure 5

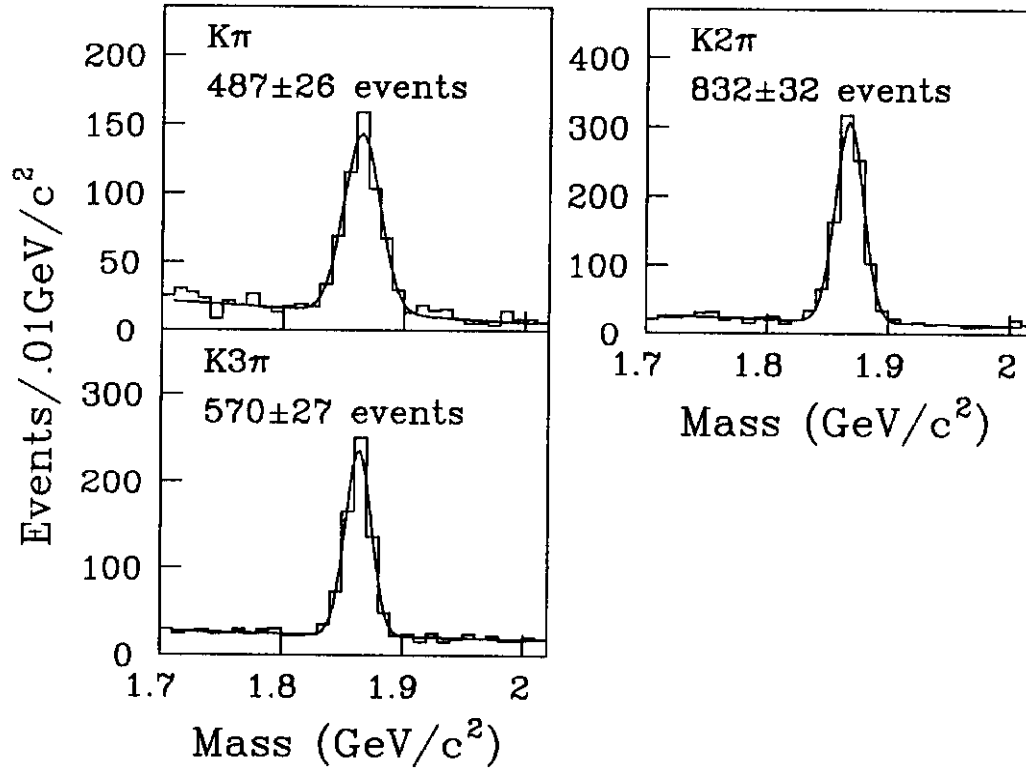


Figure 6

